

# HF SOUNDERS FOR GEOSPACE PLASMA OBSERVATIONS<sup>1</sup>

Bodo W. Reinisch

*Environmental, Earth, and Atmospheric Sciences Department, Center for Atmospheric Research, University of Massachusetts Lowell, 600 Suffolk Street, Lowell, MA 0185, USA, bodo\_reinisch@uml.edu*

## ABSTRACT

Interferometric Doppler imaging has become an integral part in radio sounding of geospace plasmas. Doppler and angle of arrival measurements have become important tools of ionospheric HF radio science. The state of the art in HF sounding and automated ionogram interpretation is reviewed in this paper.

## INTRODUCTION

Radio sounding is a well-established technique that was first deployed in the 1920's for ionospheric sounding from the ground [1]. In recent years, advanced digital sounders were developed for groundbased observations that provide detailed information about the structure and dynamics of the bottomside ionosphere [2]. These modern sounders measure more than just the time of flight and amplitude of the echoes, they also determine the arrival angle, wave polarization, and Doppler frequency. Radio sounding relies on total reflection of radio waves from plasma structures that have plasma frequencies  $f_N$  equal to the radio frequencies  $f$ . It is, therefore, not possible on the ground to receive echoes reflected from the topside ionosphere or the magnetosphere since the ionospheric F2 layer prevents all transmitted waves with frequencies  $f < f_{oF2}$  (the maximum plasma frequency) from propagating beyond the height of the F2 layer peak. The first topside ionospheric sounders [3], Alouette and ISIS [4, 5] recorded the amplitudes and echo delay times of ionospheric echoes as function of frequency in the same way it was done by the groundbased sounders of the time. The typical frequency range of the analog sounders was 0.1 to 20 MHz [6] corresponding to the plasma frequencies in the ionosphere. Recently, modern radio sounding techniques were applied to magnetospheric sounding with frequencies from 3 kHz to 3 MHz [7, 8], corresponding to electron densities of  $N_e \approx 10^5$  to  $10^{11} \text{ m}^{-3}$  since  $f_N/1\text{Hz} \approx 9 \sqrt{N_e/1\text{m}^{-3}}$ .

## PRINCIPLES OF RADIO SOUNDING

Remote sensing of space plasmas with radio waves was originally developed for ground-based ionospheric observations using different techniques: partial reflection (2-6 MHz), total reflection or radio sounding (0.1 –30 MHz), coherent scatter (10-100 MHz), and incoherent scatter (50-900 MHz). Hunsucker [9] gives a brief description of these different techniques. The discussion in this paper is limited to HF radio sounding of space plasmas. Electromagnetic waves propagate through a magnetoionic medium in the so-called free-space mode as long as  $n^2 > 0$  where  $n$  is the index of refraction. Reflection occurs where  $n = 0$  and the plasma density gradient is parallel to the wave normal [10]. Only waves with the so-called characteristic wave polarizations are solutions of Maxwell's equations [11]. The characteristic polarizations are generally right and left hand elliptical [12] with regard to the magnetic field direction. In ionospheric radio science, the left and right hand waves are usually referred to as ordinary and extraordinary waves. Solving Maxwell's equation for  $n = 0$  gives the following three reflection conditions (cutoff frequencies):

$$\begin{aligned} X = 1 & \quad \text{ordinary (O) wave} \\ X = 1 - Y & \quad \text{extraordinary (X) wave} \\ X = 1 + Y & \quad \text{Z-wave} \end{aligned} \tag{1}$$

$$X = \left( \frac{f_N}{f} \right)^2, \quad Y = \frac{f_H}{f}, \quad f_N = \sqrt{\frac{N e^2}{4\pi^2 m \epsilon_0}}, \quad f_H = \frac{e B_0}{2\pi m}.$$

$N$ ,  $e$ , and  $m$  are number density, charge, and mass of the electrons,  $\epsilon_0$  is the free space permittivity, and  $B_0$  is the earth's magnetic field. The O and Z modes have left hand, and the X mode right hand polarization with respect to the magnetic field direction. Except at high latitudes, the Z mode is rarely observed from the ground and the two prevailing modes, O and X, can be identified by the sense of rotation of the  $\mathbf{E}$  field vector. Ionosondes typically scan through frequencies

<sup>1</sup> This work was supported by AF contract F 19628-96-C-0159

from ~0.5 to 30 MHz transmitting narrow pulses into the vertical direction and measuring the echo delay time. The data can be displayed in form of an ionogram showing the echo delay as function of the sounding frequency. The echo delay  $t_d$  is usually expressed in terms of the virtual height  $h' = 0.5 c t_d$  where  $c$  is the free space speed of light. The quiet daytime ionogram in Fig. 1 was recorded at Millstone Hill, Massachusetts (42°N) and shows echoes from the E, F1 and F2 layers. This ionogram is relatively easy to interpret since the ionosphere showed almost no irregularities –there is a traveling disturbance in the F1 region - and all the echoes were returned from overhead reflection points.

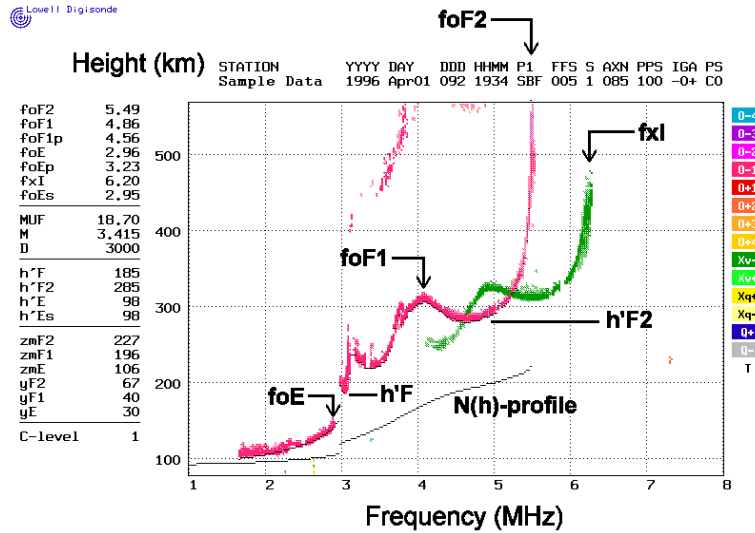


Fig. 1. Midday ionogram at Millstone Hill, MA displaying the O (red) and X (green) echo traces. Automatic scaling of the traces (black dashes at the leading edge of the traces) provides  $h'(f)$ , from which the electron density profile  $N(h)$  is calculated. The corresponding plasma frequency profile is superimposed on the ionogram. Some of the autoscaled characteristics are listed on the left.

### MODERN HF SOUNDERS

Modern sounders measure all echo parameters: echo delay time, amplitude, phase, Doppler frequency, wave polarization, and angle of arrival. Digital signal processing techniques have reduced the radiated pulse power requirements to a few hundred watts from a few kilowatts in conventional groundbased ionosondes. These measurements make it possible to determine the structure and dynamics of the reflecting plasma, and they enable the automatic scaling of the ionograms and the calculation of the vertical electron density profiles in real time. Use of turnstile antennas determines the wave polarization, i.e., it identifies the ordinary (O) and extraordinary (X) wave components, and a properly spaced array of receiving antennas can determine the angle of arrival for groundbased observations. The array dimensions are comparable to the wavelength. Space-borne sounders require three orthogonal antennas for direction finding, and amplitude and phase measurements for each antenna signal [13]. Reinisch et al. [14] have described a simple way of finding the arrival angle by using the “quadrature vectors  $\mathbf{E}_i$  and  $\mathbf{E}_q$ ” obtained from the quadrature samples of the three orthogonal signal components. The vector product  $\mathbf{E}_i \times \mathbf{E}_q$  is parallel to the wave normal, at least as long as the local plasma frequency is much smaller than the sounding frequency. These techniques produce correct arrival angles for a single arriving wave at frequency  $f$ . This is rarely the case, however, and echoes arrive simultaneously from different directions depending on the existing plasma structure. This creates complicated ionogram images with overlapping vertical and oblique O and X echoes as illustrated in Fig.2.

To correctly identify and interpret overlapping echoes in terms of plasma density and echo location it is necessary to measure the wave polarization (O or X), the arrival angle, and the Doppler shifts of the echoes together with the echo delay time, and not simply the echo amplitude (see the insert in Fig. 2). Fourier analysis of the signals at each range bin isolates the individual waves coming from different directions because of their different Doppler shifts:

$$d_j = \frac{1}{\pi} \mathbf{k}_j \cdot \mathbf{v} \quad (2)$$

Here  $\mathbf{k}_j$  is the wave vector, and  $\mathbf{v}$  is the velocity of the reflecting plasma. Applying interferometry to each spectral component determines the angles of arrival for the different echoes [15].

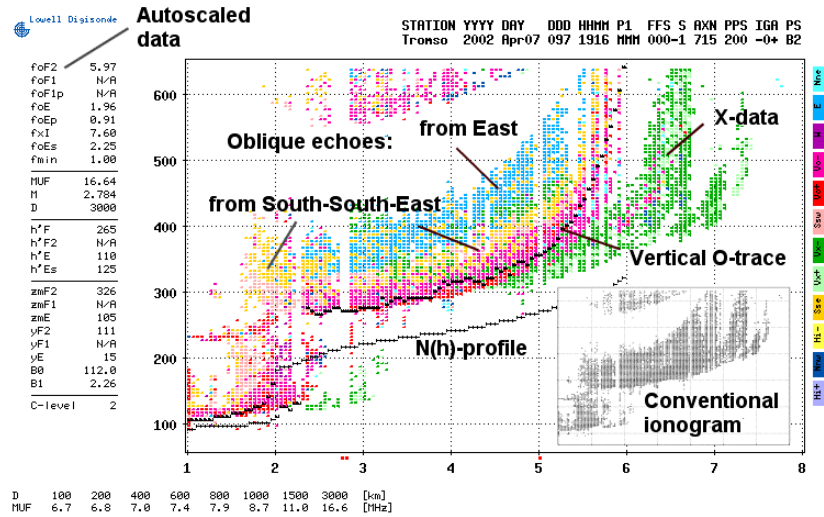


Fig. 2. Spread F ionogram at Tromso, Norway. Traces formed by echoes from the east, south-south-east, and overhead are clearly identified by the modern sounder. The autoscaled vertical O-trace (black dots) automatically generated the  $N(h)$  profile. The insert in the lower right corner shows the ionogram that conventional ionosonde would produce. The autoscaled characteristics on the left are reasonably accurate.

Similar to optical sky images, echo skymaps [2] can be constructed showing the locations of the radio sources (reflection points), each source having its own line-of-site (LOS) velocity. The velocity vector of the moving plasma is obtained from the set of LOS velocities. Some modern ionosondes calculate the velocity components in real time as illustrated in Fig. 3. The radio plasma imager (RPI) on IMAGE [16] has for the first time applied modern sounding techniques to space-borne sounding. The magnetospheric measurements are recorded in the form of plasmagrams (Fig. 4) where the virtual ranges are given in units of Earth radii,  $R_E$ .

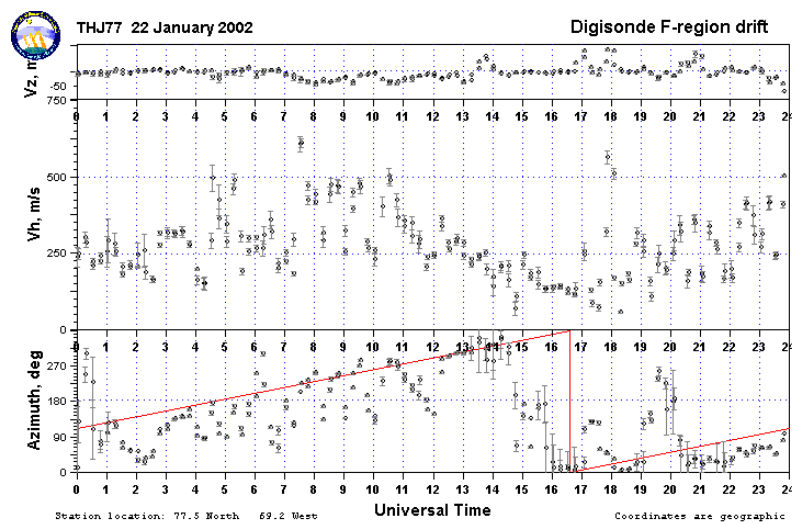


Fig. 3. Real time drift velocity at Qaanaaq, Greenland on 22 January 2002. Vertical velocity  $v_z$  (top), horizontal velocity component  $v_h$  (middle), and the azimuth of  $v_h$  (bottom) measured from geographic north. The solid (red) line in the azimuth panel gives the anti-sunward direction.

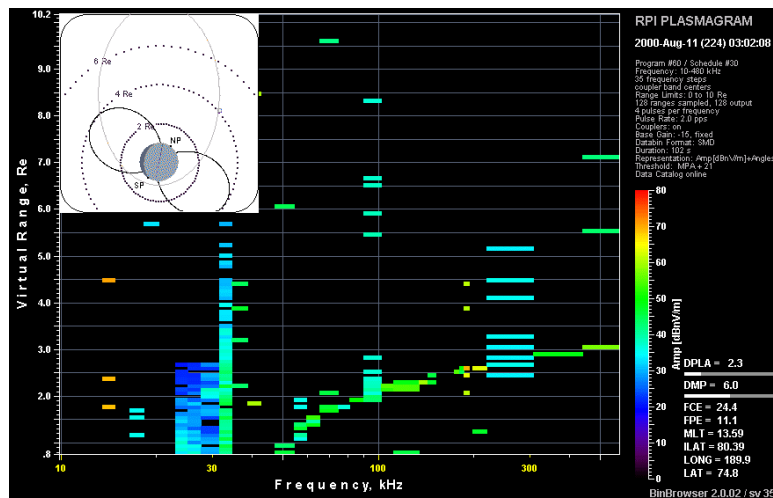


Fig.4. RPI plasmagram scanning from 30 to 600 kHz with virtual ranges up to 10  $R_E$ . An X trace from the polar cap region extends from 50 to 600 kHz. RPI transmits less than 10 W of pulse power.

A historical review of ionosonde development is given in [17].

## REFERENCES

- [1] Breit, G. and M.A. Tuve, A test for the existence of the conducting layer, *Phys. Rev.*, 28, 554-575, 1926.
- [2] Reinisch, B.W., Modern Ionosondes, in *Modern Ionospheric Science*, edited by H. Kohl, R. Rüster and K. Schlegel, European Geophysical Society, Katlenburg-Lindau, Germany, 440-458, 1996.
- [3] Franklin, C.A. and M.A. Maclean, The design of swept-frequency topside sounders, *Proc. IEEE*, 57, 897-929, 1969.
- [4] Jackson, J.E., E.R. Schmerling, and J.H. Whitteker, Mini-review on topside sounding, *IEEE Trans. Antennas Propagat.*, AP-28, 284-288, 1980.
- [5] Jackson, J.E., Alouette-ISIS Program Summary, *NSSDC Report 86-09*, National Space Science Data Center, Greenbelt, MD, 1986.
- [6] Pulinets, S.A., Prospects of topside sounding, in *WITS Handbook No. 2*, edited by C.H. Liu, SCOSTEP Publishing, Urbana, IL, 99-127, 1989.
- [7] Reinisch, B.W. et al., The Radio Plasma Imager investigation on the IMAGE spacecraft, *Space Science Reviews*, 91, 319-359, 2000.
- [8] Reinisch, B.W. et al., First Results from the Radio Plasma Imager on IMAGE, *Geophys. Res. Ltrts*, Vol. 28, 6, 1167-1169, 2001.
- [9] Hunsucker, R.D., *Radio techniques for probing the terrestrial ionosphere*, Springer Verlag, 1991
- [10] Budden K.G., *The propagation of radio waves, the theory of radio waves of low power in the ionosphere and magnetosphere*, Cambridge University Press, New York, 669 pp., 1985.
- [11] Stix, T.H., *The theory of plasma waves*, McGraw-Hill, New York, 1962.
- [12] Rawer K. and K. Suchy, *Radio observations of the ionosphere*, *Encyclopedia of Physics*, edited by S. Flüge, vol. XLIX/2, Springer Verlag, new York, 1967.
- [13] Shawhan, S.D., The use of multiple receivers to measure the wave characteristics of very-low-frequency noise in space, *Space Science Reviews*, 10, 689-736, 1970.
- [14] Reinisch et al., Radio wave active Doppler imaging of space plasma structure, *Radio Sci.*, 34, 6, 1513-1524, 1999.
- [15] Bibl, K. and B.W. Reinisch, The universal digital ionosonde, *Radio Sci.*, 13, 519-530, 1978.
- [16] Burch, J.L. et al., Views of the Earth's magnetosphere with the IMAGE satellite, *Science*, 291, 5504, 2001.
- [17] Bibl, K., Evolution of the ionosonde, *Annali Geofisica*, 41, 5-6, 667-680, 1998.